Journal of Electroanalytical Chemistry 783 (2016) 1–7

Contents lists available at ScienceDirect

Journal of Electroanalytical Chemistry

journal homepage: www.elsevier.com/locate/jelechem

Kinetic study of the hydrogen evolution reaction in slightly alkaline electrolyte on mild steel, goethite and lepidocrocite

Kristoffer Hedenstedt [a,b], Nina Simic [a], Mats Wildlock [a], Elisabet Ahlberg [b,*]

[a] AkzoNobel Pulp and Performance Chemicals, SE-445 80 Bohus, Sweden
[b] Department of Chemistry and Molecular Biology, University of Gothenburg, Kemigården 4, SE-412 96 Gothenburg, Sweden

ARTICLE INFO

Article history:
Received 30 December 2015
Received in revised form 15 October 2016
Accepted 7 November 2016
Available online 9 November 2016

Keywords:
Chlorate process
Electrocatalysis
Fe(II) surface species
Surface complexation

ABSTRACT

Hydrogen evolution is the main cathodic reaction in the sodium chlorate process. Two types of corrosion products, α-FeOOH (goethite) and γ-FeOOH (lepidocrocite), commonly found on cathodes in the industrial process, and mild steel have been investigated by electrochemical methods to determine the rate constants and transfer coefficients for the hydrogen evolution reaction. The results show that after an initial reduction of the iron oxyhydroxides the activity for hydrogen evolution from water is similar for all three surfaces. Ex situ X-ray diffractions studies were made to reveal structural changes after polarization in the hydrogen evolution region but only the bulk materials were detected. This indicates that the reduction process is limited to the surface layer. The experimental results clearly show that the first electron transfer is rate limiting and the low transfer coefficients indicate that the transition state is closer to adsorbed hydrogen than to water in solution. It is therefore suggested that the active site for water reduction is the protonated surface group $\equiv Fe(II) - OH_2^+$ and the mechanism for hydrogen evolution is discussed in the context of the general Volmer-Tafel-Heyrovsky scheme valid for metal surfaces.

1. Introduction

Mild steel has been the natural choice of cathode material in the sodium chlorate process for decades. It is a low alloyed steel with small amounts of carbon, which is cheap and gives relatively low overpotentials for the hydrogen evolution reaction (HER) [1]. Other cathodes such as Ni and Ni/Mo alloys give lower overpotentials but they are considered as poisons for the process. Nickel ions have shown to catalyse decomposition of the reaction intermediate hypochlorite in the bulk electrolyte [1,2], lowering the current efficiency and increasing the oxygen content in the cell gas leading to safety issues. There are also more viable materials but they are still not stable enough to be commercialized [1,3–10]. One drawback with the mild steel cathode is that it corrodes severely in the process and needs to be replaced more often than the anode. To prevent the corrosion and to increase the current efficiency sodium dichromate is added to the process. The chromate is reduced in situ to a chromium (III) oxide or hydroxide which efficiently hinders the reduction of hypochlorite on the cathode and acts as a corrosion inhibitor at the shut downs [1,11–19].

Previous studies of the HER on cathodes in the chlorate process have shown differences in the Tafel plots, $dE/d(\log j)$, between freshly polished and "corroded" mild steel electrodes [4,19–23]. These studies have given valuable information to the industry on the performance of the steel electrodes under process conditions. Yet, kinetic studies are lacking and the electrode surfaces need to be better characterised. Results from previous in-house studies at AkzoNobel Pulp and Performance Chemicals show that corroded cathodes from a well performing sodium chlorate plant had goethite, α-FeOOH, as the main product on the surface. Lepidocrocite, γ-FeOOH, on the other hand was found as the main corrosion product on cathodes from a plant with poor performance with regard to power consumption, see Supplementary information. Since the electrolytic power consumption of the chlorate process requires about 5 MWh per metric ton produced [18] and the yearly production is around 3.6×10^6 tons [1] it is of interest to reduce the energy required in the process, both for economic and environmental reasons.

In the present paper α-FeOOH and γ-FeOOH are produced in pure forms and evaluated towards the hydrogen evolution reaction and compared with a fresh mild steel electrode. The objectives of this paper are to determine the mechanism and reaction kinetics for hydrogen evolution on these two iron oxyhydroxides in slightly alkaline electrolyte, mimicking the surface conditions of the cathode in a chlorate cell. The overall goal is to explain the differences in performance found for these two compounds under process conditions.

* Corresponding author.
E-mail address: ela@chem.gu.se (E. Ahlberg).

http://dx.doi.org/10.1016/j.jelechem.2016.11.011

2. Experimental

Two different types of electrodes have been used in this study. Electrodeposited electrodes, where the active substances were potentiostatically deposited onto titanium substrate and carbon paste electrodes, where the active substances were synthesized as a powder and mixed with carbon paste. Both electrodes have been tested towards their activity for the hydrogen evolution reaction in slightly alkaline solution. Their activity has been tested against titanium grade 1 and polished mild steel, EN 10277–2-2008, rotating disc electrodes with geometric area 1 cm^2. The mild steel material contains <0.06% C, 0.20–0.3% Mn and <0.01% S.

A conventional three electrode single compartment cell was used with electrolyte volume 150 cm^3. The electrolyte was continuously purged with nitrogen during the measurements. A cylindrical mesh made of platinum with a geometrical surface area of 55 cm^2 and Ag/AgCl (Metrohm 6.0724.140) with 3 M KCl (Sigma Aldrich p.a.) inner electrolyte and equipped with a double junction were used as counter and reference electrodes, respectively. The potential of the reference electrode was 210 mV vs. she and all potentials are given with respect to this reference electrode.

The electrolyte solution consisted of 0.200 M Na_2SO_4 (Sigma Aaldrich p.a) at a pH set to 11 using NaOH (Merk p.a). The slightly alkaline environment was chosen to mimic hydrogen evolution in the chlorate process, where the pH at the surface increases compared with the neutral pH in the bulk solution. All water used was of 18.2 MΩ MilliQ grade and pH measurements were made with a Metrohm 827 pH meter equipped with a Unitrode combi pH electrode (6.0258.000). Two point calibration was made on daily basis using Metrohms own buffers 7.00 and 9.00. Electrochemical measurements, linear sweeps and potentiostatic impedance, were performed with a Gamry Reference 600 potentiostat. The rotator set up was built in house and the rotation speed was externally verified with a Shimpo DT-205 tachometer. Linear sweep voltammetry was performed at 5 mV/s and 2 mV step size going from positive to negative potentials. Different rotation rates were tested but the current is independent of rotation rate and the analysis was therefore made at constant rotation rate, 3000 rpm. The impedance measurements were made potentiostatically with 10 mV rms amplitude and 7 points per decade. An open circuit potentiostatic impedance measurement was always made first. From this measurement the solution resistance could be determined and was used for iR compensation. Fitting of experimental data to an equivalent circuit was conducted using a home-made program.

2.1. Electrodeposited electrodes

Both α-FeOOH and γ-FeOOH were potentiostatically deposited onto 1.0 cm^2 rotating disc electrodes made out of titanium grade 1 following the description by Martinez et al. [24]. The titanium electrode was first polished with 4000 grit SiC paper and etched in 5% HF just seconds before the deposition. The potentials used for deposition were −0.150 V for α-FeOOH and 1.000 V for the γ-FeOOH and in total 4 coulombs were passed.

2.2. Carbon paste electrodes

A second set of electrodes were prepared using synthesized material and carbon paste. The preparation of α-FeOOH and γ-FeOOH followed the recipes strictly according to Cornell and Schwertmann [25]. The synthesis resulted in wet crystals which were dried for 48 h at 65 °C. The pure powder was grinded and mixed with carbon paste (Metrohm 6.2801.020) in a mortar with a ratio of 40/60 wt%. To produce electrodes, the mixture was pressed by hand into a holder with a surface area of 0.097 cm^2. The choice of using carbon paste electrodes is due to the inactivity of carbon in the potential region of interest together with the possibility to simply add active species in the carbon matrix. Previous studies have shown the applicability of this method for studying the electrochemical behaviour of sparingly conductive materials and bulk materials [26–30].

2.3. Surface characterization

X-ray diffraction (XRD) was used to analyse the deposits as well as the synthesized iron oxyhydroxide powders. A Siemens D5000 diffractometer (Cu Kα = 1.5418 Å radiation) with an incident angle of 5° served the purpose.

Surface imaging was made with scanning electron microscopy (SEM). A Leo Ultra 55 SEM equipped with a field emission gun was used for this purpose. The inlens secondary electron detector was used for imaging and the acceleration voltage was between 2 and 3 kV.

3. Results and discussion

3.1. Electrodeposited electrodes

To investigate the stability and properties of the iron oxyhydroxide species linear sweeps were made at 5 mVs^{-1} from −0.2 V to −1.8 V

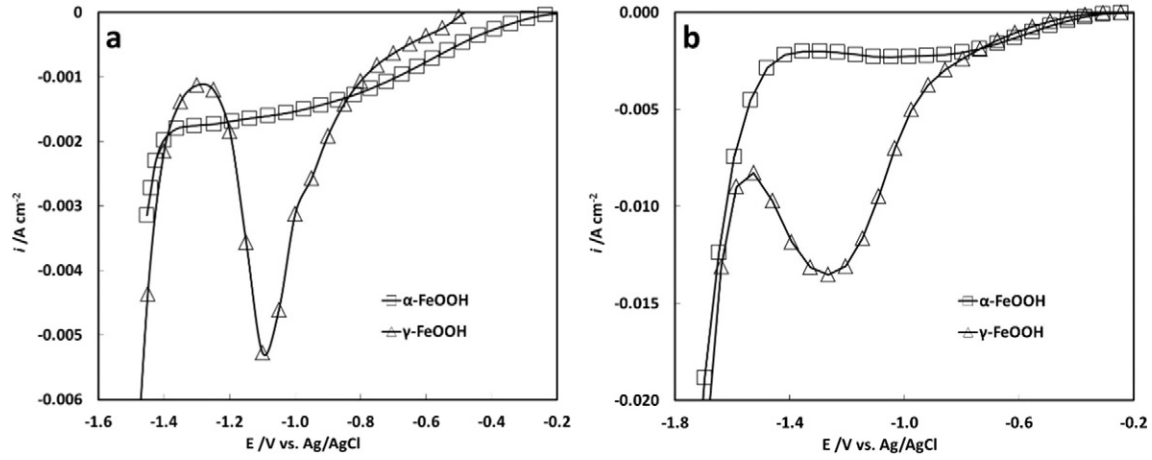

Fig. 1. Linear sweep voltammetry in negative direction at 5 mVs^{-1} for α-FeOOH (□) and γ-FeOOH (Δ) in 0.2 M Na_2SO_4 at pH 11. (a) Deposited material on titanium substrate and (b) material mixed with carbon paste.

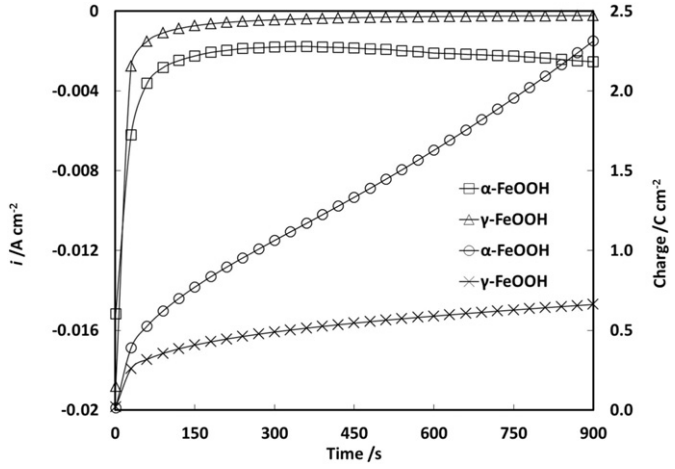

Fig. 2. Current and total charge during potentiostatic load at −1.2 V vs. Ag/AgCl for α-FeOOH (□ for current and ○ for charge) and γ-FeOOH (Δ for current and × for charge) deposited on titanium grade 1 substrate.

vs. Ag/AgCl. This is shown in Fig. 1a for deposited material and in Fig. 1b for the synthesized materials mixed with carbon paste. The currents density is smaller for the electrodeposited materials but the general behaviour is the same for the two types of electrodes. A reduction peak is observed for the gamma phase before the hydrogen evolution starts. For the alpha phase there is a cathodic current flowing related either to capacitive charging and/or reduction, but no peak is observed. Further experiments are necessary to clarify the origin of the current preceding hydrogen evolution. The reduction peak of the gamma phase has been discussed in the literature [31–34]. There is a general consensus that an Fe(II) species is formed. According to previous studies, the nature of the reduced species depends primarily on pH and magnetite is the dominant surface product for pH values where the Fe^{2+}(aq) is the main species in solution, reaction (1) [33,34].

At higher pH values $Fe(OH)_2$ is the dominant species on the surface [33]. At the pH used in the present paper, pH = 11, $Fe(OH)_2$ (aq) is the main hydrolysis product in solution and in equilibrium with solid $Fe(OH)_2$ (s) the concentration in solution is restricted to μM levels

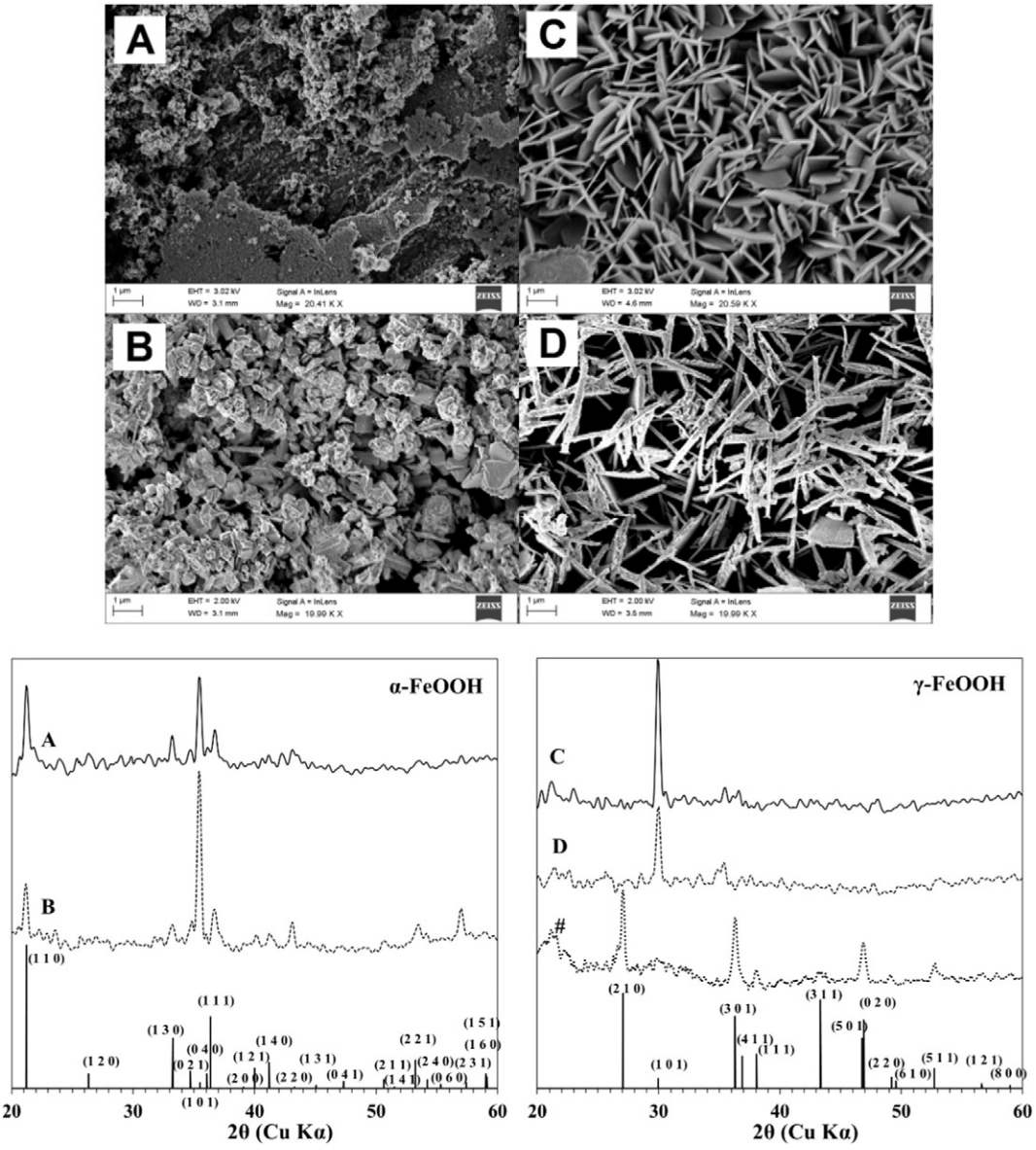

Fig. 3. SEM images of A) pristine α-FeOOH, B) α-FeOOH after 900 s at −1.2 V vs. Ag/AgCl, C) pristine γ-FeOOH and D) γ-FeOOH after 900 s–1.2 V Vs. Ag/AgCl. Below, the corresponding XRD diffractograms for the surfaces A–D together with reference diffractograms from the pure phases. XRD for scraped off material for deposited γ-FeOOH is shown in #.

[35,36]. Under these conditions the reduction can rather be considered as a solid state reduction, reaction (2).

$$Fe^{2+} + 8FeOOH + 2e^- \rightarrow 3Fe_3O_4 + 4H_2O \quad (1)$$

$$\gamma\text{-}FeOOH + e^- + H_2O \rightarrow Fe(OH)_2(s) + OH^- \quad (2)$$

The re-oxidation has also been studied and both γ-FeOOH and magnetite/maghemite were found depending on the oxidation potential and electrolyte composition [31,33,34]. For α-FeOOH mainly reductive dissolution in acid solution has been studied [37,38] and little is known about intermediate surface products in slightly alkaline solution. To test the stability of the deposited layers both electrodes were set to −1.2 V vs Ag/AgCl for 900 s and the surfaces were then analysed with SEM and XRD to compare with the pristine surface.

During the potentiostatic period the current decreases rapidly during the first 2 min. For α-FeOOH the current starts to increase again after approximately 450 s while for the γ-FeOOH the current diminishes towards zero. This results in a total charge differentiation of almost four times between the two different iron oxyhydroxide phases, where surprisingly the alpha phase induces the highest charge, Fig. 2. This could indicate that the reduction stops at the surface of the gamma phase but on the alpha phase it maintains further into the film.

Images from SEM, before and after the potentiostatic period, can be seen in Fig. 3 together with the corresponding XRD diffractograms. The XRD diffractograms show preservation of the original phases. This is in agreement with the SEM images where no major differences in the morphology of the two phases are seen although for the γ-phase the crystals seem to be slightly etched.

The single peak for the gamma phase shows a strict preferred orientation of the (1 0 1) reflection. To verify that the deposited material was indeed γ-FeOOH, the material was scraped off the electrode and analysed as a powder. The resulting diffractograms clearly show the gamma phase, Fig. 3. Also for the alpha phase preferred orientation is observed but to a lesser extent compared with the gamma phase. Preferred orientation was also observed in the work done to develop the technique of electrodeposition of the two materials [24].

After polarization no new peaks appear in the diffractogram for the gamma phase but for the alpha phase there are some additional peaks at high 2Θ angles. However, these peaks correspond well to the alpha phase and hence no new crystalline phases could be detected. The reduction to Fe(II) and dissolution of the outermost layers or small changes in the surface composition can't be excluded. Nevertheless, the major part of the phases is maintained and is therefore considered stable for the electrochemical investigation of the hydrogen evolution reaction.

Investigations of the hydrogen evolution on the deposited α- and γ-FeOOH proved to be difficult. As soon as the gas started to evolve the deposits broke off from the electrode and fell down in the cell. This was also seen in the voltammograms, where a lot of noise was detected after just a short period of time. Comparing the activity for the oxyhydroxides with the pure titanium substrate it is clear that the titanium is more active than the deposits, Fig. 4. As a consequence, the hydrogen evolution takes place on the substrate rather than on the deposits, which actually blocks the surface. Thus, the hydrogen formed on the titanium surface will break off the deposits as was observed experimentally. Instead, α- and γ-FeOOH were mixed with carbon paste for the kinetic study. The comparison between deposited material and the same material mixed with carbon paste may be influenced by the structuring of the deposited layer.

3.2. Carbon paste electrodes

The synthesized phases of α- and γ-FeOOH were analysed with XRD, Fig. 5. The XRD show the expected phases with minor preferred orientations compared with the electrodeposited species.

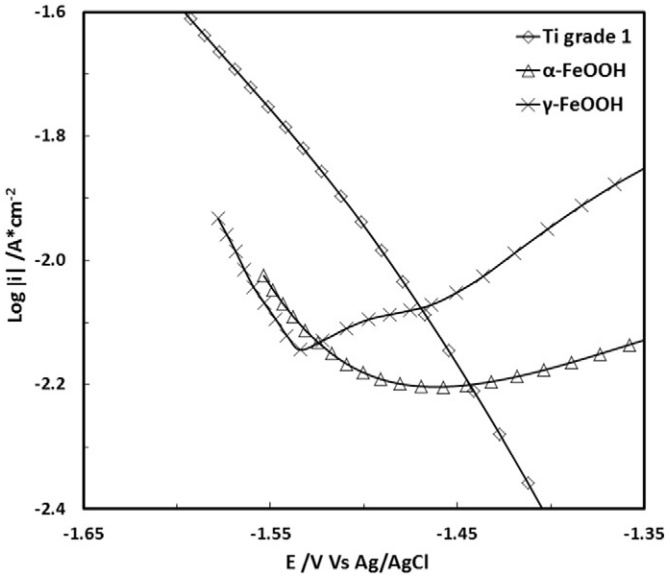

Fig. 4. Polarization diagrams for α-FeOOH (Δ) and γ-FeOOH (×) deposited on titanium compared with pure titanium grade 1 (◊) in 0.200 M Na_2SO_4 pH 11.

To fully understand and evaluate the kinetics for the hydrogen evolution reaction on the different iron oxyhydroxides, three different analyses were made using the transient current from the potential sweep, steady state current at 10 mHz measured by impedance, and charge transfer resistance obtained from impedance spectroscopy, respectively. These methods are used to give internal validity of the rate constants obtained. To calculate the kinetics from the charge transfer resistance, impedance measurements were made at different potentials. The resulting impedance was fitted to a simple equivalent circuit, Fig. 6, and the charge transfer resistance, R_{ct}, for each potential was used to calculate the kinetic current Eq. (3) [39],

$$i_{kinetic} = \frac{\eta}{R_{ct}} \quad (3)$$

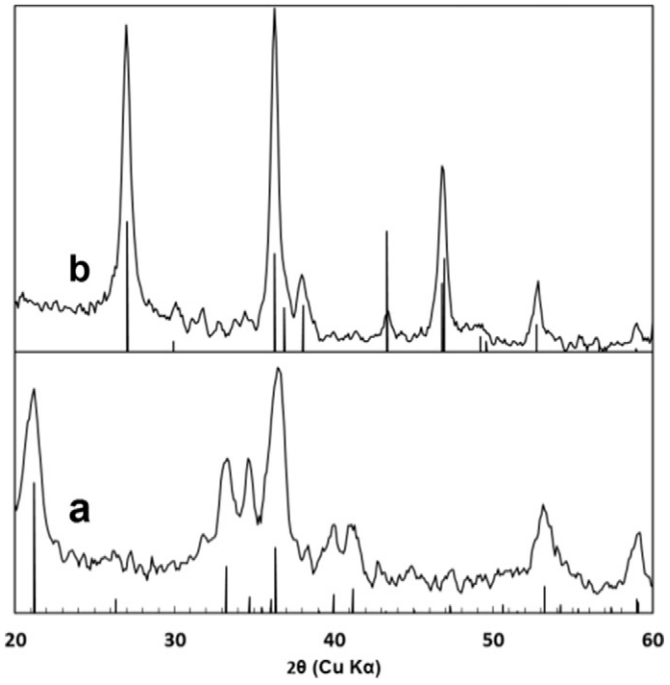

Fig. 5. XRD of synthesized pure phases of α-FeOOH (a) and γ-FeOOH (b) together with reference diffractograms. For indexation of the peaks see Fig. 3.

where η is the overpotential. The experimental data, calculated currents from the charge transfer resistance, currents from linear sweeps and steady state measurement were fitted to the theoretical Eq. (4), applicable for an irreversible electron transfer reaction, to find the rate constant k_1 and the transfer coefficient α. Temperature was set to ambient and E_0 was calculated for pH 11 and related to the Ag/AgCl reference electrode.

$$j_{kinetic} = -k_1 nFA \cdot e^{\left(\frac{-\alpha n F(E-E_0)}{RT}\right)} \quad (4)$$

F is the Faraday constant, R the gas constant, T the temperature in K, A the geometrical electrode area, n the number of electrons and E_0 the standard potential for the reaction. A summary of k_1, α and the Tafel slopes is given in Table 1. The rate constant k_1 for hydrogen evolution on α-FeOOH and γ-FeOOH depends on the state of the surface. For the first sweep in negative direction k_1 is 5 to 10 times lower, which is in line with the lower activity seen for the first sweep in Fig. 7. After the initial reduction, the three different techniques are all showing similar results. Previous studies of the hydrogen evolution reaction in alkaline electrolyte have shown kinetic constants on pure iron in the range of $3.5 \cdot 10^{-10}$ (mol m^{-2} s^{-1}) for linear sweeps [40] and $5.81 \cdot 10^{-10}$ (mol cm^{-2} s^{-1}) for steady state measurements [41]. The corresponding α values were 0.4 and 0.56, respectively.

Comparing with the results from the present study on mild steel the opposite is found, i.e. lower kinetic constants are found for the steady state measurements while higher values are obtained from the linear sweeps. The transfer coefficient α is in the present study 0.30 for both techniques.

The α- and γ-phases of the iron oxyhydroxide show similar kinetics towards hydrogen evolution. Compared to the mild steel electrode they have higher reaction constant but lower transfer coefficient, i.e. higher Tafel slopes. This gives the electrodes similar activity at low currents but as the current increases to 2–300 $mAcm^{-2}$, industrial production levels, the oxyhydroxides will have higher overpotential than mild steel.

There is one concern about the α- and γ-phases in the study when looking at log i/E graphs for the different electrodes. In Fig. 7 it can be

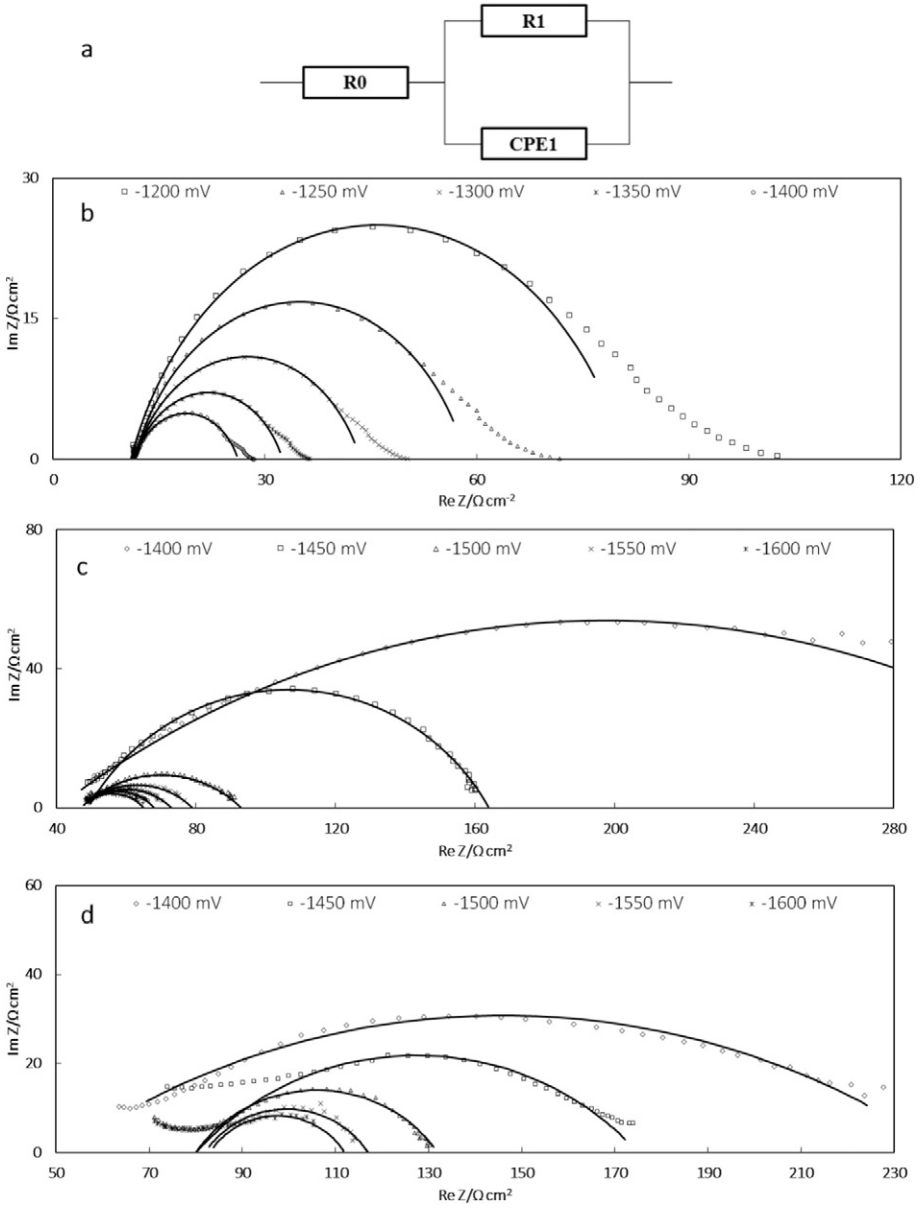

Fig. 6. Equivalent circuit used for determining the charge transfer resistance (a) and Nyqvist plots at different polarizing potentials of Mild steel (b), α-FeOOH (c) and γ-FeOOH (d). The solid lines represent the fitting to experimental data.

Table 1
Rate constant (k_1), transfer coefficient (α) and corresponding Tafel slopes modelled for α-FeOOH, γ-FeOOH and mild steel. Values are calculated from linear sweeps of pristine material (Ls 1), after polarization (Ls 2), steady state currents (i_{ss}) and the charge transfer resistance (R_{ct}).

	α-FeOOH	γ-FeOOH	Mild steel
k_1/mol cm^{-2} s^{-1}			
Ls 1	$1.7(\pm0.3)\cdot10^{-10}$	$1.6(\pm0.4)\cdot10^{-10}$	$5.2(\pm0.1)\cdot10^{-10}$
Ls 2	$2.4(\pm0.2)\cdot10^{-9}$	$3.1(\pm0.2)\cdot10^{-9}$	$6.0(\pm0.3)\cdot10^{-9}$
i_{ss}	$2.3(\pm0.3)\cdot10^{-9}$	$3.0(\pm0.2)\cdot10^{-9}$	$2.1(\pm0.2)\cdot10^{-9}$
R_{ct}	$1.4(\pm0.3)\cdot10^{-9}$	$6.5(\pm0.4)\cdot10^{-10}$	$8.0(\pm0.3)\cdot10^{-9}$
α			
Ls 1	0.22(±0.02)	0.23(±0.01)	0.30(±0.01)
Ls 2	0.23(±0.02)	0.21(±0.01)	0.30(±0.01)
i_{ss}	0.22(±0.01)	0.21(±0.02)	0.30(±0.01)
R_{ct}	0.23(±0.01)	0.23(±0.03)	0.23(±0.02)
Tafel slope /V decade^{-1}			
Ls 1	−0.258(±0.026)	−0.238(±0.018)	−0.208(±0.012)
Ls 2	−0.245(±0.032)	−0.220(±0.022)	−0.209(±0.011)
i_{ss}	−0.240(±0.028)	−0.217(±0.014)	−0.209(±0.010)
R_{ct}	−0.255(±0.019)	−0.255(±0.029)	−0.255(±0.020)

seen that neither the steady state current measurements nor the second linear sweep made after the steady state measurements are similar to the response of the pristine sample. In fact these measurements are more similar to those on the mild steel electrode. The curvature at high overpotentials is appearing due to large amounts of hydrogen gas which was seen sticking to the carbon surface leading to higher resistance that can't be compensated for. Since the phenomena of changed kinetics on the α- and γ-phases seemed to remain the electrodes were analysed with XRD to look for new phases such as magnetite or $Fe(OH)_2$ as discussed above, Section 3.1 and Fig. 3. However, no new phases could be detected indicating that the reduced surface layer is thin. The fact that the hydrogen evolution kinetics are similar for α- and γ-FeOOH after the first reduction scan supports the formation of an Fe(II) species on the surface. Since the potential is kept below −0.2 V vs. Ag/AgCl the surface will not be re-oxidized and the hydrogen evolution takes place on the reduced surface. On the solid mild steel electrode only a thin layer is formed on the surface under reducing conditions but the similar reaction kinetics also for this surface indicates that the same active sites are operating.

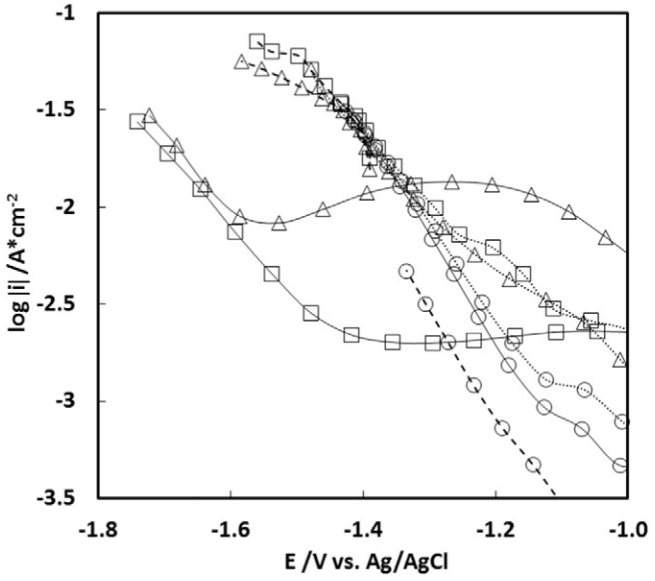

Fig. 7. Linear sweeps of the mild steel (○), α-FeOOH (□) and γ -FeOOH (Δ) electrodes before (——), during (– – – –) and after (- - - - -) steady state current measurements.

3.3. Mechanism of hydrogen evolution

It seems plausible that water reduction takes place on a reduced surface with Fe(II) sites. From the electrochemical measurements it is demonstrated that the first electron transfer is rate limiting forming adsorbed hydrogen on the hydroxide surface. Since the transfer coefficient is fairly low the transition state is closer to H_{ads} than water in solution. This implies that surface groups are reduced and there is a charge distribution in the active site with more positive charge on iron than expected for the formal oxidation number of 2. Oxides and hydroxides exhibit acid-base behaviour in aqueous solution and for goethite and lepidocrocite a summary of experimental values for the pH of zero charge (pzc) can be found in [42]. For $Fe(OH)_2$ there are no experimental pzc values available but the pzc can be estimated by the relationship between minimum solubility and pzc [43] to be around 11 [36]. The surface groups are not fully coordinated by lattice atoms and the surface charge is entirely determined by the pzc and pH of solution. The surface site ≡Fe(II)—OH^0 can be protonated or deprotonated depending on pH and are given below in the context of the 2pK model [44].

$$\equiv Fe-OH^0 + H_2O \leftrightarrow \equiv Fe-OH_2^+ + OH^- \qquad pK_{b1} \tag{5}$$

$$\equiv Fe-OH^0 + H_2O \leftrightarrow \equiv Fe-O^- + H_3O^+ \qquad pK_{a2} \tag{6}$$

The mechanism of hydrogen evolution can be formulated by assuming that the protonated surface groups are more prone to be reduced in the rate limiting electron transfer reaction forming adsorbed hydrogen on the hydroxide surface.

$$\equiv Fe-OH_2^+ + e^- \leftrightarrow \equiv Fe-OH-H_{ads} \tag{7}$$

The remaining steps can be regarded similar to the Tafel and Heyrovsky steps found for metals, reactions (8) and (9).

$$2 \equiv Fe-OH-H_{ads} \rightarrow H_2 + 2 \equiv Fe-OH^0 \tag{8}$$

$$\equiv Fe-OH-H_{ads} + H_2O + e^- \rightarrow H_2 + \equiv Fe-OH^0 + OH^- \tag{9}$$

The $\equiv Fe-OH_2^+$ groups are regenerated according to reaction (5).

4. Conclusions

In this study the electrochemical kinetics of the hydrogen evolution reaction under slightly alkaline conditions has been studied on mild steel, α-FeOOH and γ-FeOOH. The results clearly show that the first electron transfer reaction is rate limiting with Tafel slope in the range of 200–250 mV/decade. Initially the activity for the hydrogen evolution reaction on α-FeOOH and γ-FeOOH is lower than for mild steel and reduction of the oxyhydroxide takes place, presumably forming $Fe(OH)_2$ on the surface. The activity changes with time and for steady state currents the oxyhydroxides show activities similar to mild steel. The rate constant (k_1) for hydrogen evolution was found to be $(2.3 \pm 0.3)\cdot10^{-9}$ for α-FeOOH, $(3.0 \pm 0.2)\cdot10^{-9}$ for γ-FeOOH and $(2.1 \pm 0.2)\cdot10^{-9}$ mol cm^{-2} s^{-1} for mild steel. These results indicate that the reduced surface is the same on all three surfaces and that the Fe(II) surface sites are active for hydrogen evolution from water. The low transfer coefficient indicates that the first electron transfer takes place to a surface site and a mechanism is formulated in the context of surface complexation and acid base properties of the active groups.

From an industrial point of view these results suggest that start-ups of sodium chlorate plants with corroded cathodes will have high overpotentials for hydrogen evolution, which gives lower current efficiencies in the process initially. Since α-FeOOH is more readily reduced it is believed that the time to reach normal conditions in the plant is much shorter when this species is formed on the cathodes compared to cathodes with γ-FeOOH as preferred corrosion product.

Acknowledgment

Financial support from the Swedish Energy Agency, 33280-1, and Akzo Nobel Pulp and Performance Chemicals is gratefully acknowledged.

Appendix A. Supplementary data

Supplementary data to this article can be found online at doi:10.1016/j.jelechem.2016.11.011.

References

[1] H. Vogt, J. Balej, J.E. Bennett, P. Wintzer, S.A. Sheikh, P. Gallone, S. Vasudevan, K. Pelin, Chlorine oxides and chlorine oxygen acids, Ullman's Encyclopedia for Industrial Chemistry, Weinheim, Wiley-VHC Verlag, 2010.
[2] H.S. Burney, Proc. Chlor-Alkali and Chlorate Technology, R. B. Macmullin Memorial Symposium, Pennington, USA, 1999.
[3] R.D. Armstrong, M.F. Bell, Tungsten carbide catalysts for hydrogen evolution, Electrochim. Acta 23 (1978) 1111–1115.
[4] A. Cornell, D. Simonsson, Ruthenium dioxide as cathode material for hydrogen evolution in hydroxide and chlorate solutions, J. Electrochem. Soc. 140 (1993) 3123–3129.
[5] J. DeCarvalho, G.T. Filho, L.A. Avaca, E.R. Gonzales, Electrodeposits or iron and nickel-iron for hydrogen evolution in alkaline solutions, Int. J. Hydrog. Energy 14 (1989) 161–165.
[6] N. Elezovic, B.N. Grgur, N.V. Krstajic, V.D. Jovic, Electrodeposition and characterization of Fe-Mo alloys as cathodes for hydrogen evolution in the process of chlorate production, J. Serb. Chem. Soc. 70 (2005) 879–889.
[7] A. Gebert, M. Lacroix, O. Savadogo, R. Schulz, Cathodes for chlorate electrolysis with nanocrystalline Ti-Ru-Fe-O catalyst, J. Appl. Electrochem. 30 (2000) 1061–1067.
[8] E.R. Gonzales, L.A. Avaca, A. Carubell, A.A. Tanaka, G.T. Filho, The hydrogen evolution reaction on mild steel and nickel iron codeposits in alkaline media, Int. J. Hydrog. Energy 9 (1983) 689–693.
[9] J.M. Jaksic, M.V. Vojnovic, N.V. Krstajic, Kinetic analysis of hydrogen evolution at Ni–Mo alloy, Electrochim. Acta 45 (2000) 4151–4158.
[10] S. Jin, A.V. Neste, E. Ghali, S. Boily, R. Schulz, New cathode materials for chlorate electrolysis, J. Electrochem. Soc. 144 (1997) 4272–4279.
[11] A. Ahlberg Tidblad, J. Mårtensson, In situ ellipsometric characterization of films formed by cathodic reduction of chromate, Electrochim. Acta 42 (1997) 389–398.
[12] A. Ahlberg Tidblad, G. Lindbergh, Surface analysis with ESCA and GD-OES of the film formed by cathodic reduction of chromate, Electrochim. Acta 36 (1991) 1605–1610.
[13] G. Lindbergh, D. Simonsson, The effect of chromate addition on cathodic reduction of hypochlorite in hydroxide and chlorate solutions, J. Electrochem. Soc. 137 (1990) 3094–3099.
[14] G. Lindbergh, D. Simonsson, Inhibition of cathode reactions in sodium hydroxide solution containing chromate, Electrochim. Acta 36 (1991) 1985–1994.
[15] E. Müller, Über ein elektrolytisches verfawren zur gewinnung der chlor-, brom- und jodsauren salze der alkalien, Z. Elektrochem. 41 (1899) 469–473.
[16] M. Spasojevic, N. Krstajic, M. Jaksic, Electrocatalytic optimization of faradaic yields in the chlorate cell process, Surf. Techn. 21 (1984) 19–26.
[17] I. Taniguchi, T. Sekine, The influence of chromate addition on the cathodic reduction of hypochlorite ion, Denki Kagaku 43 (1975) 201–208.
[18] K. Viswanathan, B.V. Tilak, Chemical, electrochemical, and technological aspect of sodium chlorate manufacture, J. Electrochem. Soc. 131 (1984) 1551–1559.
[19] J. Wulff, A. Cornell, Cathodic current efficiency in the chlorate process, J. Appl. Electrochem. 37 (2007) 181–186.
[20] A. Cornell, G. Lindbergh, D. Simonsson, The effect of addition of chromate on the hydrogen evolution reaction and on iron oxidation in hydroxide and chlorate solutions, Electrochim. Acta 37 (1992) 1873–1881.
[21] J. Gustavsson, G. Li, C. Hummlegård, J. Bäckström, A. Cornell, On the suppression of cathodic hypochlorite reduction by electrolyte additions of molybdate and chromate ions, J. Electrochem. Sci. Eng. 2 (2012) 185–198.
[22] J. Gustavsson, L. Nylén, A. Cornell, Rare earth metal salts as potential alternatives to Cr(Vi) in the chlorate process, J. Appl. Electrochem. 40 (2010) 1529–1536.
[23] L. Nylén, J. Gustavsson, A. Cornell, Cathodic reactions on an iron RDE in the presence of Y(III), J. Electrochem. Soc. 155 (2008) E136–E142.
[24] L. Martinez, D. Leinen, F. Martín, M. Gabas, J.R. Ramos-Barrado, E. Quagliata, E.A. Dalchieleb, Electrochemical growth of diverse iron oxide (Fe_3O_4, a-FeOOH, and g-FeOOH) thin films by electrodeposition potential tuning, J. Electrochem. Soc. 154 (2007) D126–D133.
[25] M. Schwertmann, R.M. Cornell, Iron Oxides in the Laboratory, Wiley-VCH Verlag GmbH & Co, Weinheim, 1991.
[26] E. Ahlberg, J. Ásbjörnsson, Carbon paste electrodes in mineral processing: an electrochemical study of galena, Hydrometallurgy 34 (1993) 171–185.
[27] E. Ahlberg, J. Ásbjörnsson, Carbon paste electrodes in mineral processing: an electrochemical study of sphalerite, Hydrometallurgy 36 (1994) 19–37.
[28] G. Göransson, E. Ahlberg, Oxygen reduction in alkaline solution using mixed carbon paste/$Ni_xCO_{1-x}O$ electrodes, Electrochim. Acta 146 (2014) 638–645.
[29] N. Simic, E. Ahlberg, Electrochemical, spectroscopic and structural investigations of the CD:CD(II) system in alkaline media, 1. Cation effects, J. Electroanal. Chem. 451 (1998) 237–247.
[30] N. Simic, E. Ahlberg, Electrochemical, spectroscopic and structural investigations of the CD:CD(II) system in alkaline media, 2. Concentration effects, J. Electroanal. Chem. 462 (1999) 34–42.
[31] H. Antony, L. Legrand, L. Maréchal, S. Perrin, P. Dillmann, A. Chaussé, Study of lepidocrocite γ-FeOOH electrochemical reduction in neutral and slightly alkaline solutions at 25 °C, Electrochim. Acta 51 (2005) 745–753.
[32] M. Cohen, K. Hashimoto, The cathodic reduction of gamma-FeOOH, gamma-Fe_2O_3, and oxide films on iron, J. Electrochem. Soc. 121 (1974) 42–45.
[33] J. Monnier, S. Réguer, E. Foy, D. Testemale, F. Mirambet, M. Saheb, P. Dillmann, I. Guillot, XAS and XRD in situ characterisation of reduction and reoxidation processes of iron corrosion products involved in atmospheric corrosion, Corros. Sci. 78 (2014) 293–303.
[34] M. Stratmann, K. Bohnenkamp, H.-J. Engell, An electrochemical study of phase-transitions in rust layers, Corros. Sci. 23 (1983) 969–985.
[35] J.-P. Jolivet, C. Chanéac, E. Tronc, Iron oxide chemistry. From molecular clusters to extended solid networks, Chem. Commun., (2004) 481–487.
[36] C.F.J. Baes, R.E. Mesmer, The Hydrolysis of Cations, John Wiley & Sons, Inc., New York, 1976.
[37] T. Grygar, Kinetics of electrochemical reductive dissolution of iron(III) hydroxy-oxides, Collect. Czechoslov. Chem. Commun. 60 (1995) 1261–1273.
[38] U. Hasse, J. Nießen, F. Scholz, Atomic force microscopy of the electrochemical reductive dissolution of sub-micrometer sized crystals of goethite immobilized on gold electrodes, J. Electroanal. Chem. 556 (2003) 13–22.
[39] A.J. Bard, L.R. Faulkner, Electrochemical Methods — Fundamentals and Applications, second ed. John Wiley & Sons, 2001.
[40] L. Nylén, A. Cornell, Effects of electrolyte parameters on the iron/steel cathode potential in the chlorate process, J. Appl. Electrochem. 39 (2009) 71–81.
[41] M.R.G. Chialvo, A.C. Chialvo, Hydrogen evolution reaction on a smooth iron electrode in alkaline solution at different temperatures, Phys. Chem. Chem. Phys. 3 (2001) 3180–3184.
[42] M. Kosmulski, The pH-dependent surface charging and the points of zero charge, J. Colloid Interface Sci. 253 (2002) 77–87.
[43] S. Ardizzone, S. Trasatti, Interfacial properties of oxides with technological impact in electrochemistry, Adv. Colloid Interf. Sci. 64 (1996) 173–251.
[44] D.A. Dzombak, F.M.M. Morel, Surface Complexation Modeling: Hydrous Ferric Oxide, John Wiley & Sons, Inc., Canada, 1990.